Progress in Nuclear Energy 52 (2010) 258–267

Contents lists available at ScienceDirect

Progress in Nuclear Energy

journal homepage: www.elsevier.com/locate/pnucene

# Fractional scaling method applied to a pressurizer test facility

David A. Botelho [a], Paulo A.B. De Sampaio [a], Maria de Lourdes Moreira [a,*], Antonio C.O. Barroso [b]

[a] Instituto de Engenharia Nuclear (IEN/CNEN–RJ), Caixa Postal 68550, 21945-970 Rio de Janeiro, RJ, Brazil
[b] Instituto de Pesquisas Energéticas e Nucleares (IPEN/CNEN–SP), Av. Professor Lineu Prestes 2242, 05508-000 São Paulo, SP, Brazil

*Keywords:*
Fractional Scaling
Fractional Rate of Change
Fractional Change Metric
Hierarchy of Complex Systems
Scale Distortion
Information Synthesis

A B S T R A C T

Local Scaling and Fractional Scaling Analysis (FSA) have been applied at the system level to surge flow transients in a pressurizer with the purpose of sizing a 1/100 volume scale test facility. It was shown that the relation between pressure and volume displacement rates is analogous to that of generalized "effort" and "flow" in interdisciplinary analysis of complex systems. At the component level, a relation between pressurizer liquid volume and the volume displacement rates is obtained. Properly scaled outsurge transients in a full scale pressurizer have identical pressure and liquid volume histories as compared to a properly designed 1/100 volume experimental facility. FSA allows the rank of the processes quantitatively and thereby objectively in the order of their importance. For the case in analysis, surge flow dominates all other volume displacement rates (the second in importance was due to the heater). The dominant agent of pressure change in the pressurizer is that due to maximum surge flow. For similarity, the same dominant agent of change is assumed for the experiment, which permits to define its surge flow. Likewise, the heating power of the experiment, necessary to control the specified out-surge flow transient, is calculated assuming equality in the second largest agent of change, which is that due to heating.



## 1. Introduction

### 1.1. Background

This paper presents an application of Fractional Scale Analysis (Zuber et al., 2005; Wulff et al., 2005) to the pressurizer dome in the integral vessel of the International Reactor Innovative and Secure (IRIS) (Carelli, et al., 2004). The pressurizer dome is treated here as a system with two components: the vapor and the liquid volumes. The system is modeled from a holistic point of view, which means that we are looking at the whole system rather than its parts, and scaling is carried out at the system level. The system pressure is the generalized "effort" affecting simultaneously all components and it accounts not only for the fluid inventory but, more importantly, for the energy stored in the compressed fluids (Wulff et al., 2005). For a two-region pressurizer, the system pressure variation is a consequence of "volume" displacements, or generalized "flows", caused by twelve agents of change. Five of them act inside the vapor volume component and the other seven in the liquid volume. At the component level, the variation of the liquid volume is a consequence of "volume" displacements caused by nineteen types of agents of change. Twelve are derived from pressure variation and the other seven originated from liquid specific volume. There are two distinct and important system characteristics: the Fractional Rates of Change $\omega$ (FRC) that quantifies the intensity of each transfer process (agent of change) affecting the state variables in terms of what fraction of the variable total change the agent was responsible for. This serves to rank the agent impact on the system (pressurizer). The other is the Fractional Change Metric $\Omega$ for scaling the fractional change of the system state variables.

### 1.2. Purpose of the work

FSA is applied at system and component levels to find what conditions the (1/100 volume) IRIS Pressurizer Test Facility (IRIS-PTF) should obey to produce the same properly scaled depressurization history and liquid volume history as the full size IRIS. For this comparison we have used a computed outsurge transient results from a two region pressurizer model (Botelho et al., 2005).

## 2. Pressure transient

Pressure variation is considered uniform throughout the pressurizer, because the flow between the modules (regions in the pressurizer) is not choked. There are heat losses through the

* Corresponding author. Maria de Lourdes Moreira, Instituto de Engenharia Nuclear/Comissão Nacional de Energia Nuclear, RJ, Brazil. Tel.: +55 21 21733904; fax: +55 21 26082909.
*E-mail addresses:* sampaio@ien.gov.br (P.A.B. De Sampaio), malu@ien.gov.br, malu-moreira@ig.com.br (M. de Lourdes Moreira), barroso@ipen.br (A.C.O. Barroso).

0149-1970/$ – see front matter © 2009 Elsevier Ltd. All rights reserved.
doi:10.1016/j.pnucene.2009.08.004

**Nomenclature**

| | |
|---|---|
| $A$ | cross-sectional area |
| $h$ | enthalpy per unit mass |
| $h_{lv}$ | interface enthalpy per unit mass |
| $h_{\text{Nusselt}}$ | heat transfer coefficient of wall condensation |
| $L$ | volume height |
| $m$ | mass |
| $\dot{m}_{lv}$ | interface mass flow rate |
| $\dot{m}_{\text{surge}}$ | surge mass flow rate |
| $p$ | pressure |
| $\dot{Q}_{\text{heater}}$ | heating power |
| $\dot{Q}_l$ | heat balance in liquid volume |
| $\dot{Q}_{lv}$ | interface heat transfer power |
| $\dot{Q}_{\text{v}}$ | heat balance in vapor volume |
| $\dot{Q}_{wl}$ | wall heat losses from liquid volume |
| $\dot{Q}_{wv}$ | wall heat losses from vapor volume |
| $S_l$ | liquid volume wall area |
| $S_{\text{v}}$ | vapor volume wall area |
| $T$ | fluid temperature |
| $t$ | time |
| $v$ | volume per unit mass |
| $V$ | total volume of pressurizer |
| $V_l$ | liquid volume |
| $V_v$ | vapor volume |
| $\dot{V}_j$ | j$^{\text{th}}$ rate of volume change |
| $\dot{V}_j^*$ | j$^{\text{th}}$ normalize rate of volume change |
| $W_l$ | mass balance |
| $W_{\text{FL}}$ | flashing mass flow rate |
| $W_{\text{RO}}$ | rainout mass flow rate |
| $W_{\text{WC}}$ | wall condensation mass flow rate |

*Greek Symbols*

| | |
|---|---|
| $\Delta p$ | range of pressures |
| $\Delta t_{\text{ref}}$ | reference time |
| $\Delta V_{l,\ \max}$ | range of liquid volumes |
| $\Phi_j$ | rate of pressure change effect from jth agent of change |
| $\varphi_j^*$ | jth rate of pressure change scaled to include fixed ratio of fractional change rates |
| $\kappa_l$ | specific isentropic compressibility of liquid |
| $\kappa_{\text{v}}$ | specific isentropic compressibility of vapor |
| $K_{s,\ \text{syst}}$ | specific isentropic compressibility of system |
| $\Omega_p$ | Fractional Change Metric of pressure state variable |
| $\Omega_V$ | Fractional Change Metric liquid volume |
| $\omega_j$ | jth rate of fractional change |
| $\overline{\omega}_p$ | effective rate of fractional change of pressure |
| $\overline{\omega}_V$ | effective rate of fractional change of liquid volume |
| $\widehat{\omega}_j$ | j$^{\text{th}}$ ratio of rates of fractional change |

*Subscripts*

| | |
|---|---|
| FL | flashing |
| RO | rainout |
| WC | wall condensation |
| f | saturated liquid |
| g | saturated vapor |
| heat | heater power |
| i | liquid or vapor |
| j | factor of change |
| l | liquid |
| lg | liquid-steam phase change |
| t = 0 | initial value |
| v | vapor |
| 0 | initial value |

*Superscripts*

| | |
|---|---|
| * | scaled ' non-dimensional variable |
| p | changes of liquid volume due to pressure |
| v | changes of liquid volume due to specific volume |
| V | changes of liquid volume due to v and p, Eq. (67) |

metallic walls of the pressurizer in contact with external ambient air, and some heat losses through the thermal insulation of the pressurizer liquid from remaining primary fluid in the reactor vessel (Barroso et al., 2003). To compensate for heat losses and to control the pressure drop in an outsurge, a heater is provided in the liquid region, which is actuated accordingly from signals of pressure probes (Barroso and Batista Fo, 2004) and (Botelho et al., 2005). The IRIS pressurizer layout is shown in Fig. 1.

A summary of the governing equations in the liquid and vapor volumes of a pressurizer can be seen in Botelho et al., 2007. These equations are reproduced below to the benefit of reader:

$$V_v\frac{\mathrm{d}m_{\text{v}}}{\mathrm{d}t}+V_l\frac{\mathrm{d}m_l}{\mathrm{d}t}+\left(\frac{\partial \text{v}}{\partial h_{\text{v}}}\right)_p\left(m_{\text{v}}\frac{\mathrm{d}h_{\text{v}}}{\mathrm{d}t}\right)+\left(\frac{\partial \text{v}}{\partial h_l}\right)_p\left(m_l\frac{\mathrm{d}h_l}{\mathrm{d}t}\right)+\left[m_{\text{v}}\left(\frac{\partial \text{v}_l}{\partial p_l}\right)_{h_v}+m_l\left(\frac{\partial \text{v}}{\partial p}\right)_{h_l}\right]\frac{\mathrm{d}p}{\mathrm{d}t}=0$$

$$\frac{\mathrm{d}}{\mathrm{d}t}(m_{\text{v}})=W_{\text{v}}$$

$$\frac{\mathrm{d}}{\mathrm{d}t}(m_l)=W_l$$

$$\frac{\mathrm{d}}{\mathrm{d}t}(m_{\text{v}}h_{\text{v}})=\dot{Q}_{\text{v}}+m_{\text{v}}\text{v}_{\text{v}}\frac{\mathrm{d}p}{\mathrm{d}t}$$

$$\frac{\mathrm{d}}{\mathrm{d}t}(m_lh_l)=\dot{Q}_l+m_l\text{v}_l\frac{\mathrm{d}p}{\mathrm{d}t}$$

where:

$$W_{\text{v}}=W_{\text{FL}}-W_{\text{RO}}-W_{\text{WC}}-\dot{m}_{\text{lv}}$$

$$W_l=-W_{\text{FL}}+W_{\text{RO}}+W_{\text{WC}}+\dot{m}_{\text{lv}}+\dot{m}_{\text{surge}}$$

$$\dot{Q}_{\text{v}}=(W_{\text{FL}}-W_{\text{WC}})h_g-W_{\text{RO}}h_f-\dot{m}_{lv}h_{lv}-\dot{Q}_{lv}-\dot{Q}_{\text{wv}}\ \text{and}$$

$$\dot{Q}_l=(W_{\text{RO}}+W_{\text{WC}})h_f-W_{\text{FL}}h_g+\dot{Q}_{\text{heater}}\dot{m}_{lv}h_{lv}+\dot{Q}_{lv}+\dot{m}_{\text{surge}}h_{\text{surge}}-\dot{Q}_{wl}$$

So, an equation for the pressure can be readily obtained from the total volume constraint combined with mass and energy conservation equations in both volumes as:

$$\frac{\mathrm{d}p}{\mathrm{d}t}=\frac{\sum_{i=l,\text{v}}\left(\text{v}_iW_i+\left(\frac{\partial v}{\partial h_i}\right)_p(\dot{Q}_i-W_ih_i)\right)}{-\sum_{i=l,\text{v}}\left(m_i\left(\frac{\partial v_i}{\partial p}\right)_{h_i}+m_i\text{v}_i\left(\frac{\partial \text{v}_i}{\partial h_i}\right)_p\right)}\qquad(1)$$

### 2.1. Closing equations and initial conditions

Prior to a transient we assume steady-state conditions and $\dot{m}_{\text{surge}}=0$. On the interface between the vapor and liquid volumes,

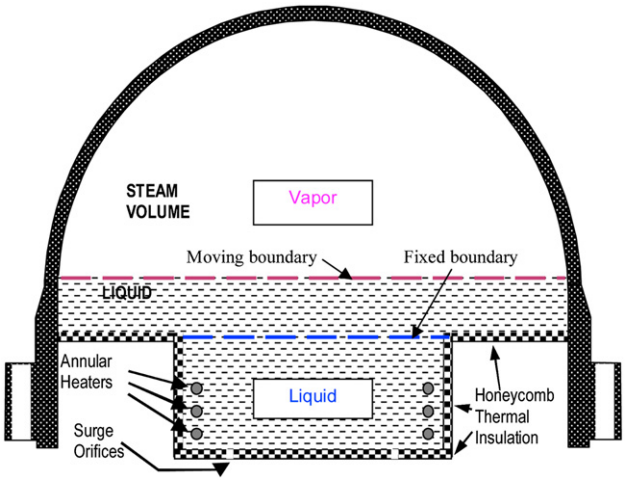


**Fig. 1.** The IRIS pressurizer layout.

the mass flow rate is calculated using a formula derived from the kinetic theory of the gases, and the heat transfer coefficient from a Nusselt number correlated for similar pressurizer experiments (Kang and Griffith, 1984).

The heat losses are calculated solving the heat conduction equation on the pressurizer walls. The wall condensation heat transfer is calculated from a Nusselt model (in Holman, 1989).

Bubble terminal velocity, as calculated by an experimental correlation (Wilson et al., 1961) or Zuber simpler formula (in Whalley et al., 1996), is assumed for all bubbles reaching the interface and used to calculate the flashing mass flow rate.

For the rainout, the velocity reached at the interface by an average falling drop immersed in the vapor fluid is used to calculate its mass flow rate.

### 2.2. Isentropic compressibility

Eq. (1) can be rewritten in the following form

$$\frac{dp}{dt} = \frac{1}{VK_{s,\mathrm{sys}}} \sum_{i=l,\mathrm{v}} \left( \mathrm{v}_i W_i + \left( \frac{\partial v}{\partial h_i} \right)_p (\dot{Q}_i - W_i h_i) \right)$$

$$= \frac{\sum \dot{V}_j}{VK_{s,\mathrm{sys}}} = \frac{\text{all agents of change j}}{\sum_{\text{all agents of change j}} \Phi_j}, \tag{2}$$

to define the individual generalized rates of volume change, $\dot{V}_j$, and the individual rates of pressure change, $\Phi_j$ for all agents of change. The denominator $K_{s,\mathrm{sys}}$ is the isentropic compressibility of the global system, i.e. the sum of the volume weighted isentropic compressibility of the aggregate sub-volumes

$$K_{s,\,\mathrm{sys}} = \sum_{i=l,\ \mathrm{v}} \frac{V_i}{V} (\kappa_s)_i \tag{3}$$

where:

**Table 1**
Mass flow rates in IRIS pressurizer.

| | $W_{WC}$ ($10^{-3}$ kg/s) | $W_{FL}$ ($10^{-3}$ kg/s) | $W_{RO}$ ($10^{-3}$ kg/s) |
|---|---|---|---|
| IRIS-P | 1.4189 | 9.7385 | 8.4217 |
| IRIS-PTF | 0.096667 | 0.48658 | 0.39096 |

**Table 2**
Heater power and interface flow at steady state.

| | $\dot{Q}_{\mathrm{heat},\ 0}$ (kW) | $\dot{Q}_{lv}$ (W) | $\dot{m}_{lv}$ (kg/s) |
|---|---|---|---|
| IRIS-P | 28.710 | 0.00 | 4.83E-9 |
| IRIS-PTF | 1.3623 | 0.00 | 4.83E-10 |

$$(\kappa_s)_i = \frac{-m_i \left( \frac{\partial \mathrm{v}_i}{\partial p} \right)_{h_i} - m_i \mathrm{v}_i \left( \frac{\partial \mathrm{v}_i}{\partial h_i} \right)_p}{V_i} \tag{4}$$

The terms in the summation bracket in Eq. (2) represent all the possible agents of change affecting the pressurizer pressure during the entire outsurge transient. These terms are functions of the mass and energy transfer terms between the two modules of the pressurizer (vapor and liquid volumes), the mass flow rate crossing the surge orifices, the energy provided by the heaters, and losses through the pressurizer walls.

Equation (2) is used to define the individual rates of volume dilatation or contraction, $\dot{V}_j$ in the vapor and liquid volumes, such that

$$\sum_{all\ j} \dot{V}_j = \sum_{i=l,\ \mathrm{v}} \left( \mathrm{v}_i\ W_i + \left( \frac{\partial\, v}{\partial\, h_i} \right)_p (\dot{Q}_i - W_i\ h_i) \right) \tag{5}$$

The individual rates of volume dilatation or contraction, $\dot{V}_i$, for each local phenomenon: surge flow, flashing, wall condensation, rainout, heat balances, and mass transfer terms through the interface between vapor and liquid are:

$$\dot{V}_0 = \dot{V}_{\mathrm{surge}} = \left( \mathrm{v}_l - \left( \frac{\partial \mathrm{v}_l}{\partial h_l} \right)_p (h_l - h_{surge}) \right) \dot{m}_{\mathrm{surge}} \tag{6}$$

$$\dot{V}_1 = \dot{V}_{l,\mathrm{WC}} = \left( \mathrm{v}_l + \left( \frac{\partial \mathrm{v}_l}{\partial h_l} \right)_p \left( h_f - h_l \right) \right) W_{\mathrm{WC}} \tag{7}$$

$$\dot{V}_2 = \dot{V}_{l,\mathrm{RO}} = \left( \mathrm{v}_l + \left( \frac{\partial \mathrm{v}_l}{\partial h_l} \right)_p \left( h_f - h_l \right) \right) W_{\mathrm{RO}} \tag{8}$$

$$\dot{V}_3 = \dot{V}_{l,\mathrm{FL}} = -\left( \mathrm{v}_l + \left( \frac{\partial \mathrm{v}_l}{\partial h_l} \right)_p (h_g - h_l) \right) W_{\mathrm{FL}} \tag{9}$$

$$\dot{V}_4 = \dot{V}_{l,\dot{Q}_l} = \left( \frac{\partial \mathrm{v}_l}{\partial h_l} \right)_p (\dot{Q}_{lv} + \dot{Q}_{\mathrm{heat},0} - \dot{Q}_{wl}) \tag{10}$$

$$\dot{V}_5 = \dot{V}_{l,lv} = \left( \mathrm{v}_l + \left( \frac{\partial \mathrm{v}_l}{\partial h_l} \right)_p (h_{lv} - h_l) \right) \dot{m}_{lv} \tag{11}$$

$$\dot{V}_6 = \dot{V}_{\mathrm{v,FL}} = \left( \mathrm{v}_v + \left( \frac{\partial \mathrm{v}_v}{\partial h_v} \right)_p (h_g - h_v) \right) W_{\mathrm{FL}} \tag{12}$$

$$\dot{V}_7 = \dot{V}_{\mathrm{v,WC}} = -\left( \mathrm{v}_v + \left( \frac{\partial \mathrm{v}_v}{\partial h_v} \right)_p (h_g - h_v) \right) W_{\mathrm{WC}} \tag{13}$$

$$\dot{V}_8 = \dot{V}_{\mathrm{v,RO}} = -\left( \mathrm{v}_v - \left( \frac{\partial \mathrm{v}_v}{\partial h_v} \right)_p \left( h_v - h_f \right) \right) W_{\mathrm{RO}} \tag{14}$$

**Table 3**
Maximum surge flow and maximum heater power.

| | $\dot{Q}_{\mathrm{heat},\ \mathrm{max}}$ (kW) | $\dot{m}_{\mathrm{surge},\ \mathrm{max}}$(kg/s) |
|---|---|---|
| IRIS-P | 1000 | −54.839 |
| IRIS-PTF1 | 13.333 | −0.73118 |
| IRIS-PTF2 | 10.0 | −0.54839 |

**Table 4**
Fractional rates of change for surge flow.

| | Resid. Time | $\Delta p\ K_{s,\ sys,\ 0}$ | $\omega_{surge}$ | $\overline{\omega}_p$ |
|---|---|---|---|---|
| | $\Delta\ t_{surge}$ (s) | – | ($10^{-3}$%/s) | ($10^{-3}$%/s) |
| IRIS-P | 851.57 | 0.12054 | −9.7422 | −8.8548 |
| IRIS-PTF1 | 638.68 | 0.12338 | −12.690 | −11.534 |
| IRIS-PTF2 | 851.57 | 0.12338 | −9.5175 | −8.6506 |

$$\dot{V}_9 = \dot{V}_{v,\dot{Q}_v} = -\left(\frac{\partial v_v}{\partial h_v}\right)_p (\dot{Q}_{lv} + \dot{Q}_{wv}) \tag{15}$$

$$\dot{V}_{10} = \dot{V}_{v,lv} = -\left(v_v - \left(\frac{\partial v_v}{\partial h_v}\right)_p (h_v - h_{lv})\right)\dot{m}_{lv} \tag{16}$$

$$\dot{V}_{11} = \dot{V}_{l,\dot{Q}_{heat}} = \left(\frac{\partial v_l}{\partial h_l}\right)_p (\dot{Q}_{heat}) \tag{17}$$

In an outsurge transient, the strongest agent of change is the surge flow. As will be shown in Tables 4 and 5 below, the maximum surge flow produces 1000 times more volume displacement as flashing, which is the local phenomenon that produces more volume displacement. The maximum heating, the next largest agent, which produces 100 times more volume displacement as flashing (and 10 times less than that of maximum surge flow), is responsible to restore the pressurizer pressure to the initial set point.

## 3. Fractional scaling on the system leveL

The normalized pressure, or fractional change of pressure, of order one, is defined by

$$0 \le p^* = \frac{p(t) - p_{\min}}{p_{\max} - p_{\min}} = \frac{p(t) - p_{\min}}{\Delta p} \le 1 \tag{18}$$

An scaled equation can be obtained directly from Eq. (2) by normalizing each dilatation rate with the effective dilatation rate of the aggregate as in (Zuber et al., 2005), i.e., the magnitudes of the algebraic sum of all active dilatation rates

$$\dot{V}_j^* = \frac{\dot{V}_j(t)}{\left|\sum_{j=0}^{11} \dot{V}_j\right|_{t=0}} \quad , \quad \left|\sum_{j=0}^{11} \dot{V}_j\right|_{t=0} \neq 0 \tag{19}$$

Equations (18) and (19) are introduced into Eq. (2) that after division by $\Delta\ p$ becomes directly

$$\frac{dp^*}{dt} = \left|\sum_{j=0}^{11} \omega_j\right|_{t=0} \sum_{j=0}^{11} \frac{\dot{V}_j^*}{K_{s,sys}^*} \tag{20}$$

where

$$K_{s,sys}^* = K_{s,\ sys}/K_{s,\ sys,\ 0}$$

Other terms in Eq. (20) are defined below.

### 3.1. Fractional rate of change (FRC)

Every agent of change is represented by a fixed Fractional Rate of Change (FRC), $\omega_{j,\ 0}$,

$$\omega_{j,0} = \frac{\dot{V}_{j,0}}{VK_{s,sys,0}\Delta p} \tag{21}$$

The FRCs $\omega_{j,\ 0}$, measure the intensity of their respective agents of change. The facility characteristic $VK_{s,\ sys,\ 0}$ and the operating parameters $\Delta\ p$ and $\dot{V}_{j,0}$ are included in the fixed Fractional Rates of Change, $\omega_{j,\ 0}$. FSA states that Fractional Change Metrics $\Omega_j = \omega_{j,\ 0} t_{ref}$ must be common to all scaled facilities of any volume size, system elasticity, surge flow rate, and initial pressure.

### 3.2. Fractional change metric for an aggregate

Following the method of fractional scaling introduced by Zuber et al., (2005), the aggregate Fractional Rate of Change, $\overline{\omega}_p$ is obtained by combining all FRCs related to pressurizing and depressurizing agents of change. The aggregate Fractional Agent of Change $|\overline{\omega}_p|$ gives the combined response rate and scales time correctly for the aggregate of all sub-volumes under the combined action of all change agents.

Depressurizing agents of change are outsurge flow, wall condensation, and heat losses, which cause fluid contraction. Pressurizing agent of change is only the heating causing fluid expansion. The effects on the vapor and liquid volumes of phenomena like rainout, flashing, and mass transfer through the vapor-liquid interface cancel each other. Thus, by summing over surge outflow and the remaining active agents of change (heat losses, wall condensation, and heating) one obtains the aggregate's Effective Fractional Rate of Change, $\overline{\omega}_p$, for the response rate of the aggregate

$$\overline{\omega}_p = \omega_{surge} + \omega_{\dot{Q}_{heat}} + \sum_{j=1}^{10} \omega_{j,0} \tag{22}$$

The Fractional Change Metric of the aggregate for a scaled time phase is then defined as $\Omega_p = |\overline{\omega}_p|\ t$ and is the measure of fractional change of a state variable (pressure) during the time phase, to which $\overline{\omega}_p$ applies.

The scaled time for the aggregate depressurization and system-level data synthesis is

$$t^* = \Omega_p = |\overline{\omega}_p| t,\ |\overline{\omega}_p| > 0 \tag{23}$$

According to Eq. (23) the scaled time $t^*$ is stretched in rapid pressure variations and compressed in slow ones, always in accordance with the net dilatation of the fluid caused by all active agents of change combined. This is the reason for large pressurizers, like that of IRIS reactor, and small test facilities, like IRIS-PTF, to have a common scaled depressurization history.

For the special case of a surge transient starting from equilibrium conditions, the summation term in Eq. (22) is zero. As

**Table 5**
Fractional rates of change of pressure.

| | Surge flow $\omega_{surge}$ $10^{-3}$/s | Wall condensation $\omega_{l,WC}$ $10^{-3}$/s | Vapor rainout $\omega_{l,RO}$ $10^{-3}$/s | Liquid flash $\omega_{l,FL}$ $10^{-3}$/s | Heat loss $\omega_{l,\ \dot{Q}_l}$ $10^{-3}$/s | Interface flow $\omega_{l,\ lv}$ $10^{-3}$/s |
|---|---|---|---|---|---|---|
| Index j | 0 | 1 | 2 | 3 | 4 | 5 |
| IRIS-P | −9.7422 | 0.00025 | 0.00149 | −.010075 | .008434 | 8.6E-12 |
| -PTF1 | −12.690 | 0.00168 | 0.00678 | −.049178 | 0.04082 | 8.39E-11 |
| -PTF2 | −9.5175 | 0.00168 | 0.00678 | −.049178 | 0.04082 | 8.39E-11 |

**Table 6**
Fractional rates of change of pressure.

| | Liquid flash $\omega_{v,FL}$ $10^{-3}$/s | Wall condensation $\omega_{v,WC}$ $10^{-3}$/s | Vapor rainout $\omega_{v,RO}$ $10^{-3}$/s | Heat loss $\omega_{v,\ \dot{Q}_v}$ $10^{-3}$/s | Interface flow $\omega_{v,\ Iv}$ $10^{-3}$/s | Heat input $\omega_{\dot{Q}_{heat}}$ $10^{-3}$/s |
|---|---|---|---|---|---|---|
| Index j | 6 | 8 | 7 | 9 | 10 | 11 |
| IRIS-P | 0.01007 | −0.00147 | −.001496 | −.007219 | −8.6E-12 | 0.88735 |
| -PTF1 | 0.04918 | −0.00977 | −.006785 | −.032733 | −8.4E-11 | 1.1558 |
| -PTF2 | 0.04918 | −0.00977 | −.006785 | −.032733 | −8.4E-11 | 0.86688 |

a consequence, $\overline{\omega}_p = \omega_{surge} + \omega_{\dot{Q}_{heat}} \approx \omega_{surge}$, because surge flow dominates.

The division of Eq. (20)by $|\overline{\omega}_p| = |\sum_{j=0}^{11} \omega_j|_{t=0}$ results:

$$\frac{dp^*}{dt^*} = \sum_{j=0}^{11} \frac{\dot{V}_j^*}{K_{s,\ sys}^*} = \sum_{j=0}^{11} \varphi_j^*,\ p^*(0) = 1 \tag{24}$$

Equation (24) is self-scaling because it has no free scaling parameter. The Fractional Change Metric $\Omega_p = |\overline{\omega}_p|\ t$ denotes the fractional change of pressure by all agents of change. The scaled variable of the jth agent of change,$\varphi_j^*$, in Eq. (24) is defined as

$$\varphi_j^* = \frac{\dot{V}_j^*}{K_{s,sys}^*} \tag{25}$$

The hierarchical order of the variables $\varphi_j^*$ is used for ranking agents of change according to their importance, while Eq. (24) has the correct time scaling for data synthesis and possibly for simulating outsurge pressure history.

The condition $|\overline{\omega}_p| > 0$ needed both for Eqs. (23) and (24) will always be met in scaling transients with a direct initiating change agent on a system that starts from steady-state conditions.

## 4. Fractional scaling: component level

At the component level, it is important that the liquid volume be also scaled properly in an experimental facility. The time derivative of the liquid volume is related to the pressure derivative as:

$$\frac{dV_l}{dt} = v_l \frac{dm_l}{dt} + m_l \left(\frac{\partial v}{\partial h_l}\right)_p \frac{dh_l}{dt} + m_l \left(\frac{\partial v}{\partial p}\right)_{h_l} \frac{dp}{dt} \tag{26}$$

The substitution of the mass and energy conservation equations in the liquid and Eq. (4) (with $i = l$) into Eq. (26) results

$$\frac{dV_l}{dt} = B_l - (\kappa_{s,l} V_l) \frac{dp}{dt} \tag{27}$$

where

$$B_l = \left[v_l - \left(\frac{\partial v}{\partial h_l}\right)_p h_l\right] W_l + \left(\frac{\partial v}{\partial h_l}\right)_p \dot{Q}_l \tag{28}$$

In view of Eqs. (6) through (17), Eq. (2) and Eq. (28), Eq. (27) can be written as

$$\frac{dV_l}{dt} = \sum_{j=0}^{5} \dot{V}_j + \dot{V}_{11} - \frac{\kappa_{s,l} V_l}{V K_{s,sys}} \sum_{j=0}^{11} \dot{V}_j \tag{29}$$

The liquid volume is a component state variable (effort). The normalized liquid volume, or fractional change of liquid volume, of order of unity, is defined as

$$0 \le V_l^* = \frac{V_l(t) - V_{l,min}}{V_{l,max} - V_{l,min}} = \frac{V_l(t) - V_{l,min}}{\Delta V_{l,max}} \le 1 \tag{30}$$

where $V_{l,\ max}$, $V_{l,\ min}$ are the maximum and minimum liquid volumes, respectively.

One can obtain the volume scaled equation directly by normalizing each dilatation rate with the effective dilatation rate of the aggregate, i.e., the magnitudes of the algebraic sum of all (active) dilatation rates (see Eq. (19)).

Equation (19) is introduced into Eq. (29) that after division by $\Delta V_{l,\ max}$ becomes directly:

$$\frac{dV_l^*}{dt} = \frac{\left|\sum_{j=0}^{11} \dot{V}_j\right|_{t=0} \left(\sum_{j=0}^{5} \dot{V}_j^* + \dot{V}_{11}^*\right)}{\Delta V_{l,max}} - \frac{\left|\sum_{j=0}^{11} \dot{V}_j\right|_{t=0} \kappa_{s,l,0}^* V_l^*}{V K_{s,\ sys,\ 0}^*} \sum_{j=0}^{11} \dot{V}_j^* \tag{31}$$

Eq. (31) can be written as

$$\frac{dV_l^*}{dt} = \left|\overline{\omega}_V\right| \times \left(\sum_{j=0}^{5} \varphi_j^{*V} + \varphi_{11}^{*V} - \sum_{j=0}^{11} \varphi_j^{*p}\right) \tag{32}$$

The scaled variable of the j$^{th}$ agents of change, $\varphi_j^{*V}$ and $\varphi_j^{*p}$, in Eq. (32) depends on the FRCs of all actives agents of change as:

$$\varphi_j^{*V} = \frac{\omega_{j,0}^V}{|\overline{\omega}_V|} V_j^* \tag{33}$$

and

$$\varphi_j^{*p} = \frac{\omega_{j,0}^p}{|\overline{\omega}_V|} \frac{\kappa_{s,l}^*\ V_l^*}{K_{s,sys}^*} \dot{V}_j^* \tag{34}$$

The FRCs of all actives agents of change are:

**Table 7**
Fractional rates of change ratios for pressure.

| | Wall condensation $\widehat{\omega}_{l,WC}$ | Vapor rainout $\widehat{\omega}_{l,RO}$ | Liquid flash $\widehat{\omega}_{l,FL}$ | Heat loss $\widehat{\omega}_{l,\ \dot{Q}_l}$ | Interface flow $\widehat{\omega}_{l,\ Iv}$ | Heat input $\widehat{\omega}_{\dot{Q}_{heat}}$ |
|---|---|---|---|---|---|---|
| Index j | 1 | 2 | 3 | 4 | 5 | 11 |
| IRIS-P | .000026 | .001536 | −.010341 | .000866 | 8.8E-13 | 0.09108 |
| -PTF1 | .000132 | .005347 | −.038753 | .003217 | 6.6E-12 | 0.09108 |
| -PTF2 | 0.00018 | .007129 | −.051671 | .004289 | 8.8E-12 | 0.09108 |

**Table 8**
Fractional rates of change of liquid volume.

| | Surge flow $\omega^V_{\text{surge}}\ 10^{-3}$/s | Wall condensation $\omega^V_{l,\text{WC}}\ 10^{-3}$/s | Vapor rainout $\omega^V_{l,\text{WC}}\ 10^{-3}$/s | Liquid flash $\omega^V_{l,\text{WC}}\ 10^{-3}$/s | Heat loss $\omega^V_{l,\ \dot{Q}_l}\ 10^{-3}$/s | Interface flow $\omega^V_{l,\ lv}\ 10^{-3}$/s |
|---|---|---|---|---|---|---|
| Index j | 0 | 1 | 2 | 3 | 4 | 5 |
| IRIS-P | −1.3854 | .000036 | 0.00021 | −0.00143 | 0.00120 | 1.2E-12 |
| -PTF1 | −1.8256 | 0.00024 | 0.00098 | −0.00707 | 0.00587 | 1.21E-11 |
| -PTF2 | −1.3692 | 0.00024 | 0.00098 | −0.00707 | 0.00587 | 1.21E-11 |

$$\omega^{\text{v}}_{j,\ 0} = \begin{cases} \frac{\dot{V}_{j,\ 0}}{\Delta V_{l,\ \max}},\ j = 0,\cdots,5,\ \text{and}\ j = 11 \\ 0,\ \text{otherwise} \end{cases} \tag{35}$$

$$\omega^{p}_{j,0} = \frac{\kappa_{s,l,0}\dot{V}_{j,0}}{VK_{s,\text{sys},0}},\ j = 0,\cdots,11 \tag{36}$$

The Aggregate Fractional Rate of Change $\overline{\omega}_V$ is defined below.

### 4.1. Aggregate fractional change metric for liquid volume

Following the method of fractional scaling introduced by Zuber et al., (2005), the aggregate Fractional Rate of Change, $\overline{\omega}_V$ is obtained by adding all positive FRCs related to pressurizing agents of change to the sum all negative FRCs related to depressurizing agents of change. The aggregate Fractional Agent of Change $|\overline{\omega}_V|$ gives the correct aggregate response rate and scales time correctly for the aggregate of all "processes" under the action of all agents of change combined. It includes the action of all agents of change, which are active during the scaled time phase.

Contracting agents of change are outsurge flow, wall condensation, and heat losses, which cause fluid contraction. Expanding agent of change is heating which causes overall fluid expansion. The effects on liquid volume of phenomena like rainout, flashing, and mass transfer through the vapor-liquid interface cancel each other. Thus, by summing over surge outflow and the remaining active agents of change (heat losses, wall condensation, and heating), or by scaling according to Eq. (31), one obtains the aggregate's Effective Fractional Rate of Change, $\overline{\omega}_V$, for the response rate of the aggregate processes

$$\overline{\omega}_V = \omega^{\text{v}}_{\text{surge}} + \omega^{\text{v}}_{\dot{Q}_{\text{heat}}} + \sum_{j=1}^{5}\omega^{\text{v}}_{j,0} - \omega^{p}_{\text{surge}} - \omega^{p}_{\dot{Q}_{\text{heat}}}$$
$$-\sum_{j=1}^{10}\omega^{p}_{j,\ 0} = \omega^{V}_{\text{surge}} + \omega^{V}_{\dot{Q}_{\text{heat}}} + \sum_{j=1}^{10}\omega^{V}_{j,\ 0} \tag{37}$$

where

$$\omega^V_j = \omega^{\text{v}}_j - \omega^p_j \tag{38}$$

as can be seen from Eqs. (35) and (36).

The Fractional Change Metric of the aggregate processes for a scaled time phase is then defined as $\Omega_V = |\overline{\omega}_V|\ t$ and is the measure of fractional change of a state variable (liquid volume) during the time phase, to which $\overline{\omega}_V$ applies. The Fractional Change Metric is negative during depressurization and positive for a pressure excursion when net heating (heating minus wall condensation and heat losses) overwhelms outsurge flow. If the Effective Fractional Rate of Change $\overline{\omega}_V$ is close to zero for a time phase, then the Fractional Change Metric also approaches $\Omega_V \approx 0$, and the associated time phase has nearly constant liquid volume. This occurs in the time phase when the surge flow returns to zero, after pressure control is achieved and the heating is just that necessary to compensate for wall condensation and heat losses through the walls of pressurizer.

The scaled time for the aggregate processes on liquid volume and component-level data synthesis is

$$t^* = \Omega_V = |\overline{\omega}_V|t,\ |\overline{\omega}_V| > 0 \tag{39}$$

where the time counts from the beginning of the time phase. According to Eq. (39) the scaled time $t^*$ is stretched in rapid and compressed in slow liquid volume changes, always in accordance with the net dilatation of the fluid caused by all active agents of change combined. This is the reason for large pressurizers, like that of IRIS reactor, and small test facilities, like IRIS-PTF, to have a common scaled liquid volume history.

Division of Eq. (32) by $|\overline{\omega}_V|$ and using Eq. (39) gives

$$\frac{dV^*_l}{dt^*} = \sum_{j=0}^{5}\varphi^{*V}_j + \varphi^{*V}_{11} - \sum_{j=0}^{11}\varphi^{*p}_j,\ V^*_l(0) = 1 \tag{40}$$

Equation (40) is self-scaling because it has no free scaling parameter. The Fractional Change Metric $\Omega_V = |\overline{\omega}_V|\ t$ denotes the fractional change of liquid volume by all agents of change. Time $t^*$ in Eq. (40) is stretched or compressed according to the net dilatation caused by all agents of change active during a time phase, as explained below Eq. (39).

Equation (40) has the correct time scaling for data synthesis and possibly for simulating outsurge liquid volume history. Again the condition $|\overline{\omega}_V| > 0$ needed both for Eq. (39) and Eq. (40) will be met in scaling transients with a direct initiating change agent on a system that starts from steady-state conditions. To be similar to IRIS pressurizer within the FSA framework, a scaled experiment must have the same dominants FRCs of surge flow and heating as that of IRIS pressurizer. From Eqs. (6) and (21), the FRC of surge flow is defined as:

$$\omega_{\text{surge}} = \frac{\left(\text{v}_l - \left(\frac{\partial \text{v}}{\partial h_l}\right)_p (h_l - h_{\text{surge}})\right)\dot{m}_{\text{surge,max}}}{VK_{s,\ sys,\ 0}\Delta p} \tag{41}$$

From Eqs. (17) and (21), the FRC of heating is defined as

$$\omega_{\text{heat}} = \frac{\left(\frac{\partial \text{v}}{\partial h_l}\right)_p (\dot{Q}_{\text{heat,max}})}{VK_{s,\text{sys},0}\Delta p} \tag{42}$$

**Table 9**
Fractional rates of change of liquid volume.

| | Liquid flash $\omega^V_{\text{v,FL}}\ 10^{-3}$/s | Wall condensation $\omega^V_{\text{v,WC}}\ 10^{-3}$/s | Vapor rainout $\omega^V_{\text{v,RO}}\ 10^{-3}$/s | Heat loss $\omega^V_{\text{v},\ \dot{Q}_v}\ 10^{-3}$/s | Interface flow $\omega^V_{\text{v},\ lv}\ 10^{-3}$/s | Heat input $\omega^V_{\dot{Q}_{\text{heat}}}\ 10^{-3}$/s |
|---|---|---|---|---|---|---|
| Index j | 6 | 8 | 7 | 9 | 10 | 11 |
| IRIS-P | -.002753 | .000401 | .000409 | .001973 | 2.3E-12 | 0.12619 |
| -PTF1 | -.013595 | 0.00270 | .001876 | .009049 | 2.32E-11 | 0.16628 |
| -PTF2 | -.013595 | 0.00270 | .001876 | .009049 | 2.32E-11 | 0.12471 |

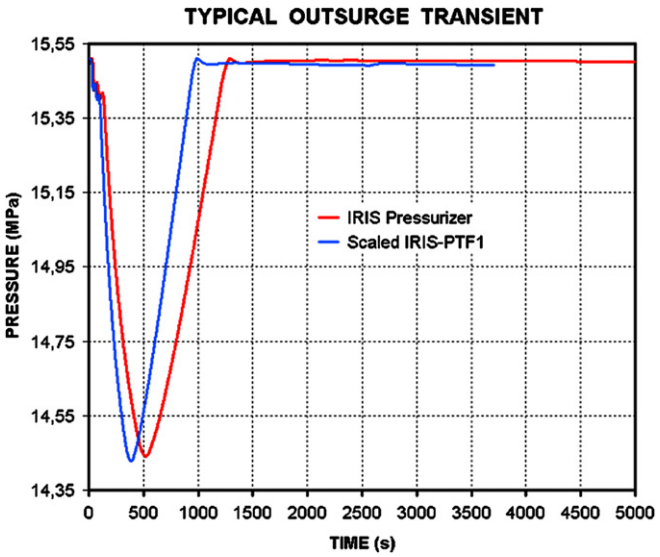


**Fig. 2.** Calculated IRIS-P and–PTF1 Depressurizations: scaled facility effects do not preserve out-surge flow time.

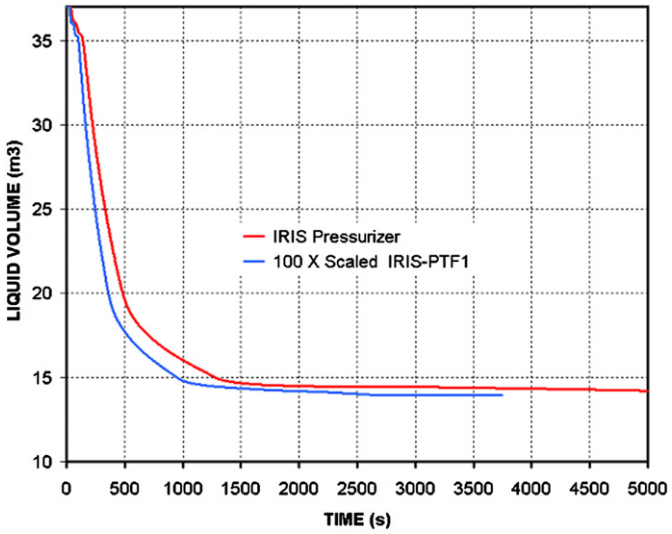


**Fig. 4.** Calculated IRIS-P and–PTF1 Liquid Volume Variations: scaled facility effects do not preserve time of liquid volume variation.

As the experiment has the same pressure, same thermodynamic properties, same system elasticity and same pressure range as IRIS pressurizer, it results from Eqs. (41) and (42) that for similarity it is necessary that the surge mass flow rate and the heating power keep the same proportion of the volume ratio.

## 5. Application

FSA at the system level is applied here in two ways, namely for establishing a process hierarchy and assessing scale distortions on the basis of Fractional Rate of Change (FRC) and for data synthesis on the basis of the Fractional Change Metric. The case analyzed was the IRIS pressurizer (IRIS-P) and IRIS-PTF, an experimental test facility that is being designed to test IRIS pressurizer performance and safety, whose volume is 1/100 of that of IRIS pressurizer. The basic transient studied was a typical outsurge transient in IRIS pressurizer (Barroso and Batista Fo, 2004).

The FRC-based hierarchy of agents of change, or transfer processes across system boundaries is an objectively quantified alternative and a step forward, from the expert opinion based Phenomena Identification and Ranking Table (PIRT). Moreover, the FRCs serves to identify and quantify scale distortion. The graph $p^*(|\Omega_p|) = p^*(t^*_{\text{surge}})$ should reveal whether the fractional change of pressure $p^*$ during outsurge tests is the same at the same value of the Fractional Change Metrics of outsurge, $\Omega_p$, regardless of IRIS pressurizer and test facility size and actual outsurge time. By the same token, the graph $V_l^*(|\Omega_V|) = V_l^*(t^*_{\text{surge}})$ should reveal whether the fractional change of liquid volume $V_l^*$ is the same at the same value of the Fractional Change Metrics of outsurge,$\Omega_V$. Congruence of respective curves $p^*(|\Omega_p|)$ and $V_l^*(|\Omega_V|)$ indicates that the (out)-surge flow governs the entire transient and that system volume, system elasticity, (dominated by saturated liquid volume in pressurizer) maximum outsurge flow, maximum heating power, initial liquid volume, and initial pressure are properly scaled; differences reveal scale distortions. The initial slopes of $p^*(|\Omega_p|)$ and $V_l^*(|\Omega_V|)$ should be always $(-1)$.

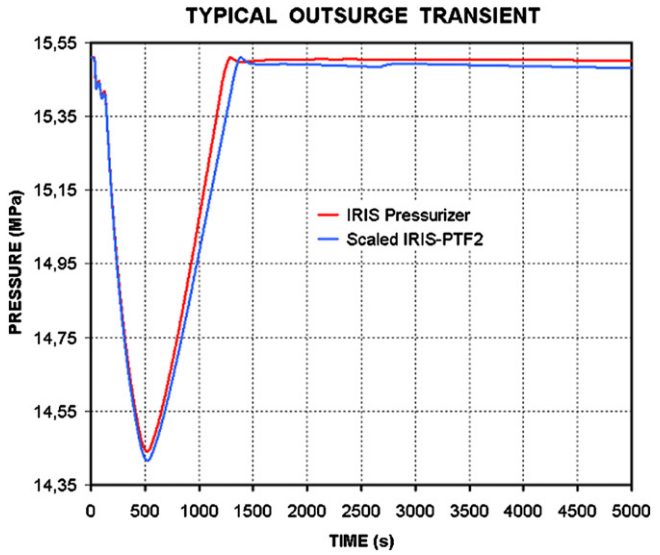


**Fig. 3.** Calculated IRIS-P and -PTF2 Depressurizations: facility effects are scaled to preserve out-surge flow time.

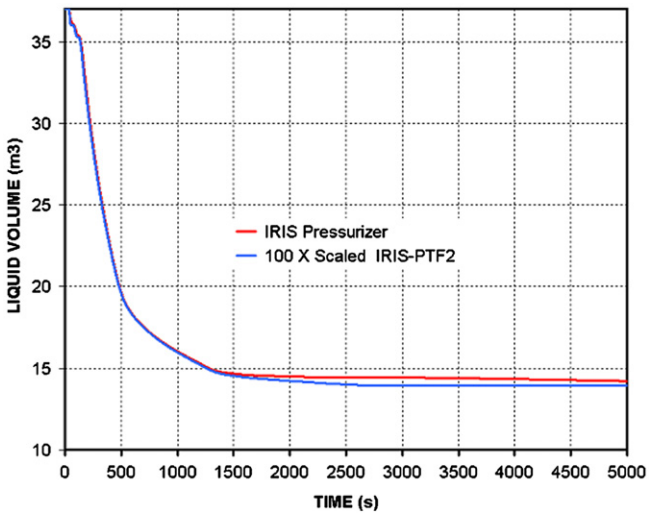


**Fig. 5.** Calculated IRIS-P and–PTF2 Liquid Volume Variations: facility effects are scaled to preserve time of liquid volume variation.

### 5.1. Initial conditions of pressurizer

Table 1 presents estimates of mass flow rates due to local phenomena of wall condensation, flashing, and rainout in IRIS-P and IRIS-PTF at steady state condition.

Due to the equality of thermal constants, the bubble terminal velocity in the liquid volume, if calculated using the Zuber formula (in Whalley et al., 1996) would be the same in IRIS-P and IRIS-PTF. The interface area ratio in IRIS-P and in IRIS-PTF is 21.5. In a calculation, with same bubble terminal velocity, the flashing mass flow rate ratio in IRIS-P and in IRIS-PTF would also be 21.5. Based on Eq. (15), the flashing mass flow rate ratio in IRIS-P and in IRIS-PTF is $(9.7385/0.4866) = 20$ (see Table 1), which is very close to the value that would be obtained using the Zuber formula. From Table 1, the rainout mass flow rate in IRIS-P divided by that in IRIS-PTF is $(8.4217/0.3901) \approx 21.6$, which is very close to the interface area ratio in IRIS-P and in IRIS-PTF.

Table 2 exhibits the heater power necessary to compensate wall condensation and wall losses, interface heat, and interface mass flow rate, at steady state conditions, and the maximum interface mass flow rate.

Table 3 exhibits the maximum surge mass flow rate in a out-surge transient and the maximum heating provided by the heater control system.

The out-surge transient in IRIS-PTF1 has a maximum mass flow rate and maximum heater power that are 1/75 of that of IRIS-P. The maximum surge flow rate of an out-surge transient in the experiment is such that the dominant FRC of surge flow given by Eq. (40) in IRIS-PTF2 is equal to that in IRIS-P. The maximum heating power in the experiment is such that the FRC for heating given by Eq. (41) in IRIS-PTF2 be equal to that in IRIS-P. Therefore, the maximum surge flow ratio and the maximum heating power in IRIS-PTF2 keep the same volume ratio of 1/100 in relation to IRIS-P.

### 5.2. Establishing process hierarchy and assessing scale distortion

The outsurge flow leaving the system is the dominant agent of change. Table 4 lists associated numerical values of the maximum and aggregate fractional rate of change, $\omega_{\text{surge}}$, Eq. (41), and $\overline{\omega}_p$, Eq. (22). Also shown in Table 4 are the residence time, or turn-over time, $\Delta t_{\text{surge}} = V/\dot{V}_{\text{surge}}$, and the fractional volume compression, $\Delta p\ K_{s,\ sys,\ 0}$. At the surge volume rate, $\dot{V}_{\text{surge}}$, to displace the control volume $V$, it takes one residence time.

It can be seen in Table 4 that the residence time dominates the inverse of $\omega_{\text{surge}}$, the FRC of maximum surge flow in both facilities of different sizes, when the same fluid is used at the same pressure. The fractional volume compression $\Delta p\ K_{s,\ sys,\ 0}$ is the fractional reduction of fluid volume when it is adiabatic compressed by $\Delta p$.

From Eq. (41) it can be demonstrated that the inverse of $\omega_{\text{surge}}$ is the product of the fractional volume compression times the residence time, or $(1/\omega_{\text{surge}}) = (\Delta p\ K_{s,\ sys,\ 0})\ \Delta t_{\text{surge}}$. This relationship can be readily verified using the data in Table 4. As the fractional volume compression $\Delta p\ K_{s,\ sys,\ 0}$ is small, this explains why the residence time dominates the inverse of $\omega_{\text{surge}}$.

Tables 5 and 6 exhibit the FRCs of pressure in Eq. (20) for the three facilities (IRIS-P, IRIS-PTF1 and IRIS-PTF2) that are active (although their sum is zero) at the start of the out-surge transient, together with the FRC of maximum surge flow and maximum heat input that are reached some time after the start of the transient. The surge flow leads and is followed by heat input provided by the pressurizer heater control system.

Table 7 exhibits the $\widehat{\omega}_j = \omega_j/\omega_{\text{surge}}$, the ratio of some FRCs to the surge flow (maximum) FRC, $\omega_{\text{surge}}$. The ratios $|\widehat{\omega}_j|$ can be ordered in a hierarchy. A criterion, such as $|\widehat{\omega}_j| > 0.1$, is used to establish that only the surge out-flow and input heating are important agents of change, the others are unimportant.

Tables 8 and 9 exhibit the FRCs of liquid volume) in Eqs. (35) and (36) for the three facilities (IRIS-P, IRIS-PTF1 and IRIS-PTF2 that are active (although their sum is zero) at the start of the out-surge transient, together with the FRC of maximum surge flow and maximum heat input that are reached some time after the start of the transient.

The criterion for scale distortion cannot be tighter than is permitted by the compound of pertinent experimental uncertainties, manufacturing tolerances and operational uncertainties, or else no important process can ever be found to be without scale distortion. The firs two rows of results in Tables 5 and 6 show that the out-surge depressurization processes of importance in IRIS-PTF1 are distorted, because the difference between the corresponding important FRCs of surge out-flow (30%) and input heating (30%) are both greater than 10%. Nevertheless, in IRIS-PTF2, the first and the last rows in Tables 5 and 6 show no out-surge depressurization processes of importance that is distorted, because the difference between the two corresponding important

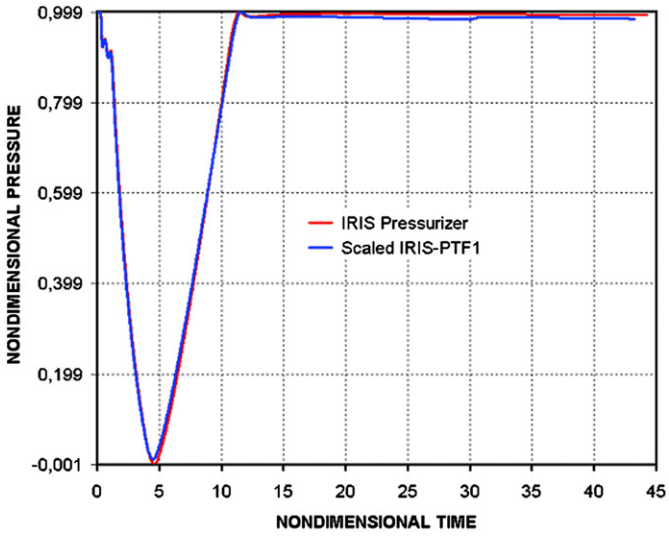


**Fig. 6.** Scaled out-surges in IRIS-P and IRIS-PTF1: effects of surge mass flow rate on time of out-surge flow are scaled.

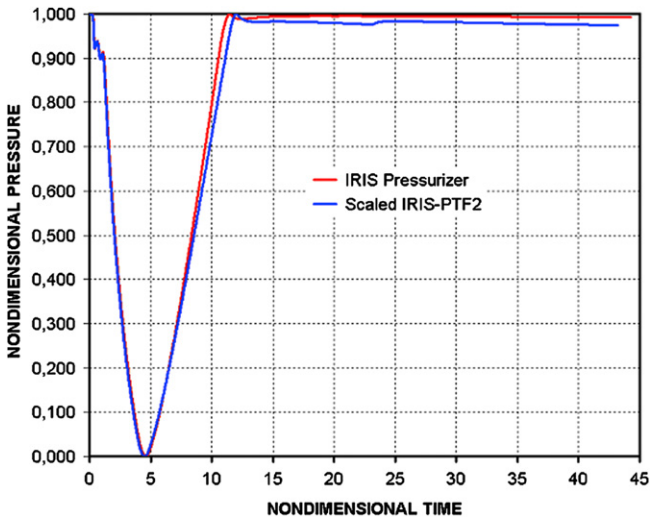


**Fig. 7.** Scaled out-surges in IRIS-P and IRIS-PTF2: effects of surge mass flow rate on time of out-surge flow are scaled.

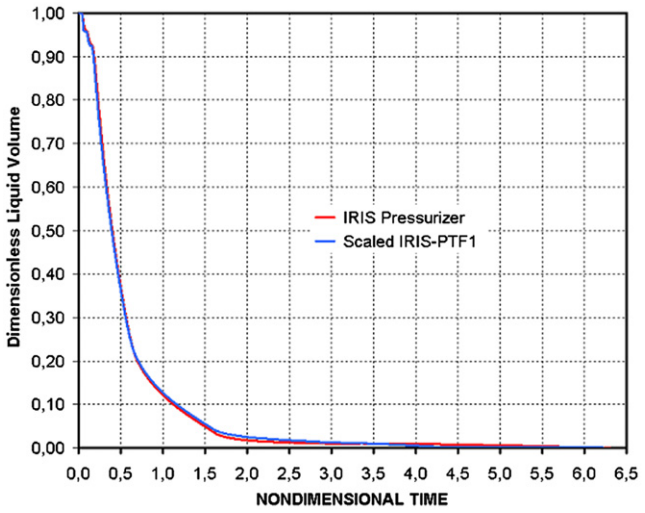


**Fig. 8.** Scaled out-surges in IRIS-P and IRIS-PTF1: effects of liquid volume on time of liquid volume variation are scaled.

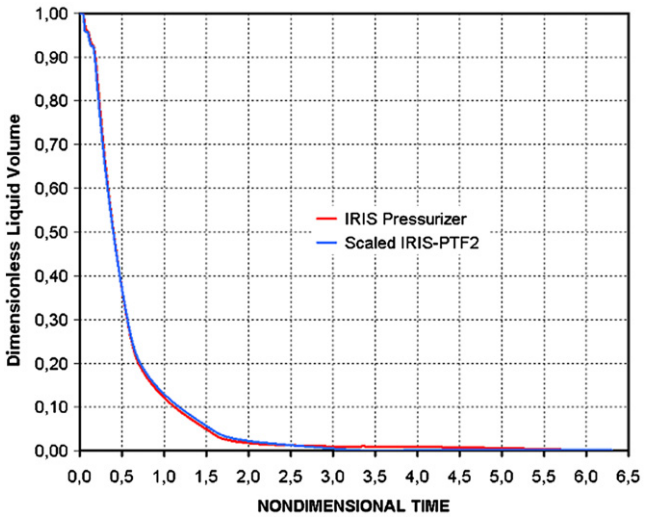


**Fig. 9.** Scaled out-surges in IRIS-P and IRIS-PTF2: effects of liquid volume on time of liquid volume variation are scaled.

FRCs, surge out-flow (2.36%) and input heating (2.36%) are both less than 10%.

From the agents of change for liquid volume in Tables 8 and 9 we see again that the surge flow leads and is followed by heat input provided by the pressurizer heater control system.

The first two rows of results in Tables 8 and 9 show that the out-surge depressurization processes of importance are distorted in IRIS-PTF1, because the difference between the two corresponding important FRCs, surge out-flow (32%) and input heating (32%) are both greater than 10%. Nevertheless, in IRIS-PTF2, the first and the last rows of results in Tables 8 and 9 show no out-surge depressurization processes of importance that is distorted, because the difference between the two corresponding important FRCs, surge out-flow (1.18%) and input heating (1.19%) are both less than 10%.

### 5.3. Data synthesis

Figs. 2 and 3 show, in currently prevailing and familiar format, calculated typical out-surge pressure histories, i.e., pressure versus out-surge time, for IRIS pressurizer (IRIS-P) and 1/100 volume scaled pressure test facilities (IRIS-PTF1 and IRIS-PTF2). The corresponding liquid volume histories, i.e., liquid volumes versus out-surge time are shown in Figs. 4 and 5.

Figs. 2 and 3 present the effects of facility sizes on pressure history. Scaled IRIS-PTF1 surge flow level and pressure control system did not preserve time for out-surge transient, because $|\omega_{surge}|$ is 0.0097422/s for IRIS-P and 0.012690/s for IRIS-PTF1 (Table 5), which is 30% more, and thus outside the accepted uncertainty range of surge flow determination (>10%).

Figs. 4 and 5 present the effects of facility sizes on liquid volume histories. Again, time scaling is not preserved in Fig. 4 for IRIS-PTF1 because $|\omega^V_{\text{surge}}|$ is 0.0013854 in IRIS-P and 0.0018256 in IRIS-PTF1, but is nearly preserved in IRIS-PTF2, because now $|\omega^V_{\text{surge}}|$ is 0.0013692 (Table 8). As can be seen in Fig. 5, the initial 1/100 volume ratio in IRIS-PTF2 is almost preserved. Evidently, scaled IRIS-PTF2 surge flow level and pressure control system nearly preserved pressure and time for out-surge transient, because $|\omega_{\text{surge}}|$ is 0.0095175/s for IRIS-PTF2 (Table 5), which is 2.36% less, close and within the accepted uncertainty range of surge flow determination.

The Fractional Rates of Change (FRC) in Tables 5 and 6 were used to calculate the FRC of the aggregate, $\overline{\omega}_p$ in Table 4, to form the Fractional Change Metric $\Omega_p = |\overline{\omega}_p|\ t$ and scale the time of the calculated transient in Figs. 2 and 3 according to Eq. (24). The pressure was scaled according to Eq. (35). This leads to the plots of $p^*(\Omega_p)$ in Figs. 6 and 7, which shows the effects of scaling parameters $\widehat{\omega}_j$.

### 5.4. Scaling of surge mass flow rate

For IRIS-PTF the effect of out-surge mass flow rate (also of heater power) on pressure is scaled, because the two curves in Figs. 6 and 7 almost collapse into one, even though the times of out-surge differ by 25% in Fig. 2. For IRIS-PTF the effect of out-surge mass flow rate and of heater power on liquid volume is also scaled, because the two curves in Figs. 8 and 9 almost collapse into one, even though the times of out-surge differ by 25% in Fig. 4.

Nevertheless, the more pronounced shape differences between the IRIS-PTF1 curves in Figs. 2 and 4 suggest dissimilar processes during out-surges in which the mass flow rates (and heater power) are not scaled according to the pressurizer volume ratio of 1/100, as in IRIS-PTF2. The convergence between the IRI-PTF2 and IRIS-P curves in Figs. 3 and 5 is a consequence of the almost agreement between the important FRCs in IRIS-P and IRIS-PTF2. Thus, for pressure and liquid level effects, IRIS-PF2 is similar to the IRIS pressurizer.

The Fractional Rates of Change (FRC) in Tables 7 and 8 were used to form the Fractional Change Metric $\Omega_V = \overline{\omega}_V\ t$ and scale the time of the calculated transient in Figs. 4 and 5 according to Eq. (40). This leads to the plots of $V_l^*(\Omega_V)$ in Figs. 8 and 9, which shows the effects of scaling parameters $\widehat{\omega}^V_j$.

## 6. Conclusions

We have applied Fractional Scaling Analysis (FSA) at the system-level, first on the basis of Fractional Rates of Change $\omega_j$ (FRC) to identify, quantify and prioritize in the order of their impact on all transfer processes responsible for system depressurization (see Tables 5–7), and secondly on the basis of the Fractional Change Metric $\Omega_p$ to synthesize computer calculated data (compare Figs. 2 and 3 with Figs. 6 and 7). We have demonstrated quantitatively for a typical out-surge in IRIS

pressurizer and a test installation being designed, called IRIS-PTF of 1/100 volume, that the surge flow is the leading agent of change for out-surge depressurization. It turned out that the absolute value of the out-surge flow-related Fractional Change Metric $\Omega_{\text{surge}} = t^*$, alone synthesizes the pressure history.

We have used local scaling and acknowledge the role that it plays in the calculation of the heating power of the experiment, once the size and the surge flow data of the experiment are defined.

We also have applied Fractional Scaling Analysis (FSA) at the component-level, first on the basis of Fractional Rates of Change $\omega_j^V$ (FRC) to identify, quantify and prioritize in the order of their impact on all transfer processes responsible for liquid volume variation (see Tables 8 and 9), and secondly on the basis of the Fractional Change Metric $\Omega_V$ to synthesize computer calculated data (compare Figs. 4 and 5 with Figs. 8 and 9). We have demonstrated quantitatively for a typical out-surge in IRIS pressurizer and the test installation IRIS-PTF, that the surge flow is also the leading agent of change for liquid volume variation. It turned out that the absolute value of the out-surge flow-related Fractional Change Metric $\Omega_{\text{surge}} = t^{*V}$, alone synthesizes the liquid volume history.

We have found that a successful data synthesis requires that the surge flow (and heating power) be scaled in the same proportion to the pressurizer and test installation volume ratio. A successful data synthesis also requires a reliable and complete system specification and test data and is therefore performed most efficiently and reliably during testing, when data can be easily retrieved as part of a computer simulation.

## References


Barroso A.C.O., Batista Fo. B. D., "Refining the Design of the IRIS Pressurizer". Proceeding of the 5th International Conference on Nuclear Option in Countries with Small and Medium Electricity Grids, Dubrovnik, Croatia (2004).

Barroso A.C.O., Batista Fo. B.D., Arone I.D., Macedo L.A., De Sampaio P.A.B., and Morais M., "IRIS Pressurizer Design". Proceedings of the ICAPP, Cordoba, Spain, Paper 3227 (2003).

Botelho, D.A., De Sampaio, P.A.B., Moreira, M.L., Barroso, A.C.O., 2005. Simulation of IRIS Pressurizer Out-surge Transient using Two and Three Volumes Simulation Models. International Nuclear Atlantic Conference (INAC), Santos, SP, Brazil.

Botelho D.A., De Sampaio P.A.B., Moreira M.L., and Barroso A.C.O., "Application of Fractional Scaling Analysis and Local Scaling to Design a Test Facility of IRIS Pressurizer". Paper 7373 of the Proceedings of the ICAPP 2007, Nice, France, May 13–18 (2007).

Carelli, M.D., Conway, L.E., Oriani, L., Petrovi, B., Lombardi, C.V., Ricotti, M.E., Barroso, A.C.O., Collado, J.M., Cinotti, L., Todreas, N.E., Grgi, D., Moraes, M.M., Boroughs, R.D., Ninokata, H., Ingersoll, D.T., Oriolo, F., 2004. The design and safety features of the IRIS reactor. Nuclear Engineering and Design 230, 151–167.

Holman, J.P., 1989. Heat Transfer. McGraw-Hill Book Company, Singapore.

Kang, S.-W., Griffith, P., 1984. Pool heat transfer in a simulated PWR pressurizer. Transactions of the ANS 46, 845–847.

Whalley, P.B., 1996. Two-Phase Flow and Heat Transfer. Oxford University Press, New York.

Wilson, F., Grenda, R.J., Patterson, J.F., 1961. Steam volume fraction in a bubbling two-phase mixture. Transactions of the American Nuclear Society 4, 356–357. section 37.

Wulff W., Zuber N., Rohgati U.S., and Catton I., "Application of Fractional Scaling Analysis (FSA) to Loss of Coolant Transients (LOCA), Part 2: System Level Scaling For System Depressurization". The 11th International Topical Meeting on Nuclear Reactor Thermal-Hydraulics (NURETH-11). Pope's Palace Conference Center, Avignon, France, October 2–6, 2005.

Zuber N., Wulff W., Rohgati U.S., and Catton I., "Application of Fractional Scaling Analysis (FSA) to Loss of Coolant Transients (LOCA), Part 1: Methodology Development". The 11th International Topical Meeting on Nuclear Reactor Thermal-Hydraulics (NURETH-11). Pope's Palace Conference Center, Avignon, France, October 2–6, 2005.